Arch. Metall. Mater., Vol. 61 (2016), No 3, p. 1671–1676

DOI: 10.1515/amm-2016-0270

A.P.I. POPOOLA*, N. MALATJI*, O.S.I FAYOMI*,**

FABRICATION AND INVESTIGATION OF THERMAL AND WEAR PROPERTIES OF ZINC NOVEL COATINGS REINFORCED WITH NANO-Al_2O_3 AND Cr_2O_3 PARTICLES

The study of the thermal, wear and corrosion properties of developed nanocomposite coatings of Zn-Al_2O_3 and Zn-Cr_2O_3 was carried out. The coatings were produced by electrodeposition technique from chloride acidic bath. Laboratory tube furnace was used for the thermal analysis. The wear test was performed using CETR tribo-tester dry reciprocating tester. The hardness properties were investigated using diamond base Dura microhardness tester. Scanning electron microscope (SEM) affixed with energy dispersive spectrometry was used to study the morphological characteristics, before and after wear deformation. The corrosion degradation behavior was observed using linear polarization technique in 3.5% NaCl. In all the interaction, the effects of the incorporated Al_2O_3 and Cr_2O_3nanoparticulates on zinc rich coatings were found to have an excellent influence on the wear, corrosion and thermal stability properties. The fabrication and properties exhibited by the alloys were therefore found to be satisfactory and shows good predictability and applicability.

Keywords: Microstructure, corrosion, nanocomposite coatings, thermal stability, tribology

1. Introduction

Zinc alloy/nanocomposite coatings have received a great research interest in the past years. This is due to their enhanced performance in harsh environments compared to the traditional Zn coatings. Metals and metal oxides, carbides, nitrides or borides are incorporated into the metal matrix to enhance the quality of the coatings. These nano-materials possess unusual and excellent properties that are not exhibited in the traditional bulk material of the same kind. The properties include good corrosion and wear resistance, biocompatibility, thermal stability and self-lubrication [1]-[3]. Electrodeposition is one of the techniques that is used for incorporation of these particles into a metal matrix. Some advantages electrodeposition has over other deposition techniques include low cost, flexibility and ease of operation, high production rate, easily available equipment and less contamination [4].

Simple oxides such as Al_2O_3, TiO_2, ZrO_2, CeO_2 and SiO_2 are commonly used due to their ease of availability. These oxides can be incorporated into plain Zn matrix or Zn alloy [4]-[10]. Al_2O_3 nanoparticles were found to improve electrochemical behavior of Zn-Ni when they were incorporated within the optimal concentrations. It was established that these particles have significant effect on the surface morphology of the coatings [6]. Reference [7] found that the hardness was also improved due to the incorporation of the particles aided by ultrasound conditions. Research has shown that incorporation of Cr_2O_3 into a metal matrix yields positive results on the mechanical and thermal properties such as microhardness, wear resistance and thermal stability. However, no significant effect was found on the electrochemical behavior of the matrix [11].

There is no sufficient information in the available literature that provides insight about incorporation of Al_2O_3 and Cr_2O_3 nanoparticles into Zn matrix and their special properties. Therefore, this research aims to fabricate Zn-Al_2O_3 and Zn-Cr_2O_3 nanocomposite coatings and compare the properties that can be impacted by these nanoparticles on Zn matrix for advanced industrial applications.

2. Experimental

TABLE 1

Bath Composition and Operating parameter

Composition	g/L	Parameters	
$ZnCl_2$	150	Cathode	Mild steel
KCl	50	Anode	Zn
Boric Acid	30	Temperature	250C
Glycine	30	pH	3.8
Thiorea	10	Current	1.5A
Al_2O_3	2.5-10		
Cr_2O_3	2.5-10		

Zn-Al_2O_3 and Cr_2O_3 nanocomposite coatings were fabricated by electrodeposition technique. Table 1 above shows the bath composition and operating conditions for fabrication of the composites. Sectioned mild steel (25x40x1 mm) cathodes were polished by using 180 and

* SURFACE ENGINEERING RESEARCH CENTRE, DEPARTMENT OF CHEMICAL, METALLURGICAL & MATERIALS ENGINEERING, TSHWANE UNIVERSITY OF TECHNOLOGY, P.M.B X680, PRETORIA, SOUTH AFRICA

** DEPARTMENT OF MECHANICAL ENGINEERING, COVENANT UNIVERSITY, P.M.B. 1023, CANAAN LAND, OTA, NIGERIA

Corresponding author: ojosundayfayomi3@gmail.com, Popoolaapi@tut.ac.za, doublen.malatji@gmail.com

400 grit SiC emery papers to remove the unwanted material on the substrate. Degreasing followed by suspending the samples into ethanol, dipped into 1M hydrochloric acid to activate the surface and then rinsed in water before plating. Two Zinc (99.9%) plates were used as anodes. The solutions for plating were prepared a day prior to the tests. To ensure even dispersion and prevent agglomeration of the nanoparticles of Al_2O_3 and Cr_2O_3 which were added into the bath, the solutions were mechanically stirred for 18hrs using a magnetic stirrer. Sigma Aldrich spherical Al_2O_3 and frosty like shaped Cr_2O_3 powders (Fig. 1) with average diameter of 50 and 100 nm respectively were used with no prior treatment from the supplier. Adjustment and keeping the pH at 3.8 was made by addition of hydrochloric acid or sodium hydroxide. All the electroplating tests were conducted under ambient conditions at a plating time of 20 min and of speed of 300 rpm. The plated samples were then rinsed in water for 5 seconds and then left to air dry. The thickness of the produced coatings was measured to be about 25 μm. Vega Tescan scanning electron Microscopes (SEI mode) equipped with Energy Dispersive Spectrometry was used to study the surface morphology and content of the incorporated particles in the deposits.

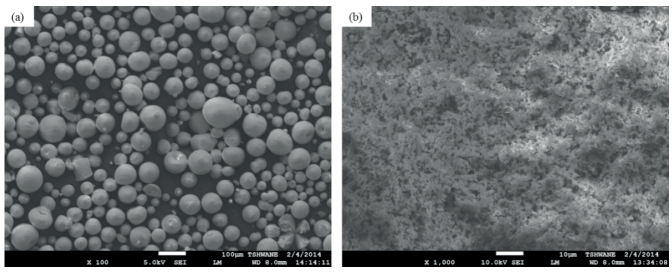

Fig. 1. SEM image of received (a) Al_2O_3 and (b) Cr_2O_3 powders

Potentiodynamic polarization technique was used to investigate the corrosion behavior of the coatings in 3.65% NaCl environment using μAUTOLAB Pontentiostat/ Galvanostat. The polarization measurements were carried at a scanning rate of 0.01 V/s at a potential range of -1.5 to 1.5V. Corrosion parameters from polarization studies were obtained by extrapolations of the anodic and cathodic Tafel slopes. Saturated calomel electrode was used as a reference and graphite served as a counter electrode. A diamond indenter microhardness tester was used to investigate the microhardness of the deposits. An average of three measurements in different locations of the sample was taken to ensure correct and accurate values that represent the specimen. The samples were exposed to annealing temperature of 250 °C in a laboratory tube furnace. The duration range of the heat treatment was 0.5, 2 and 16 hours to evaluate the thermal stability of the coatings with respect to time. Microhardness evolution of the coatings was followed according to the duration range. CETR tribo-tester was used to study the wear characteristics of the coatings under dry reciprocating conditions. A normal load of 5N and a velocity of 2 m/s at a sliding distance of 2 mm were used as operating variables. The coefficient of friction was continually recorded for 1000s in all the tribology tests. . Dry abrasion rig machine was used to determine the percentage wear mass loss under dry sliding conditions using silica sand as a wearing medium at a speed of 200 rev/ min for 60 s. The initial mass of the samples were weighed before the tests and the final masses were recorded after the dry sliding. These values were used to determine the percentage wear mass loss.

TABLE 2

Sample Codes and Description

Sample Codes	Sample Description
ZA1	Zn-5g/L Al_2O_3
ZA2	Zn-10g/L Al_2O_3
ZC1	Zn-10g/L Cr_2O_3
ZC2	Zn-20g/L Cr_2O_3

3. Results and discussion

3.1. Morphological studies

The surface morphologies of Zn, Zn-Al_2O_3 and Zn-Cr_2O_3 nanocomposite coatings are shown in Figure2. Pure Zn coating shows a flake-like crystalline structure (Fig. 2a) with coarse grains and surface defects (micro holes and pores). These defects can serve as weak sites for the degradation of the quality of the coatings when they are exposed to trying environments. ZA1 (Fig. 2b) and ZC2 (Fig. 2c) follow a similar arrangement but exhibit uniform and compact microstructure with smaller crystal grains. Incorporation of nanoparticles into a metal matrix induces grain refinement by impeding the growth of the crystals. Therefore, the modification of the morphological characteristics of the Zn coatings can be attributed the incorporation of Al_2O_3 and Cr_2O_3 nanoparticles into matrix. EDS results as shown in Figure 4 confirmed the presence of Al_2O_3 (2.2 wt %) and Cr_2O_3 (7.38 wt %) in the coating. The cross-section micrographs are also presented in Figure 3 and show that the particles are incorporated into the Zn matrix.

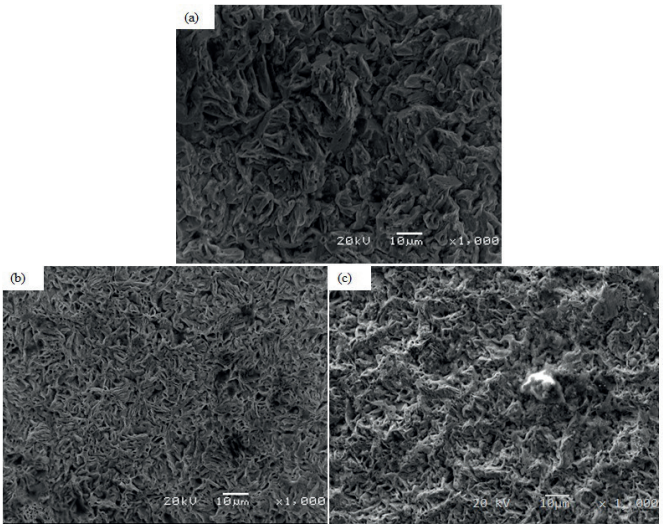

Fig. 2. SEM micrographs (a) Zn coating (b) Zn-5g/L Al_2O_3 coating and (c) Zn-20g/L Cr_2O_3 coating

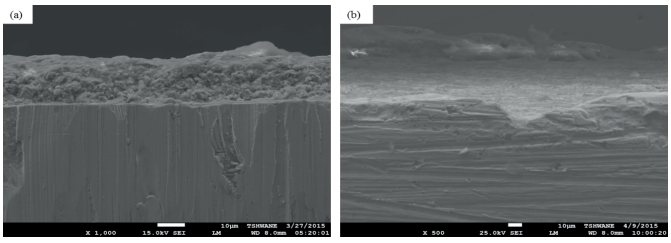

Fig. 3. SEM images of the cross section (a) ZA1 and (b) ZC2 nanocomposite coatings

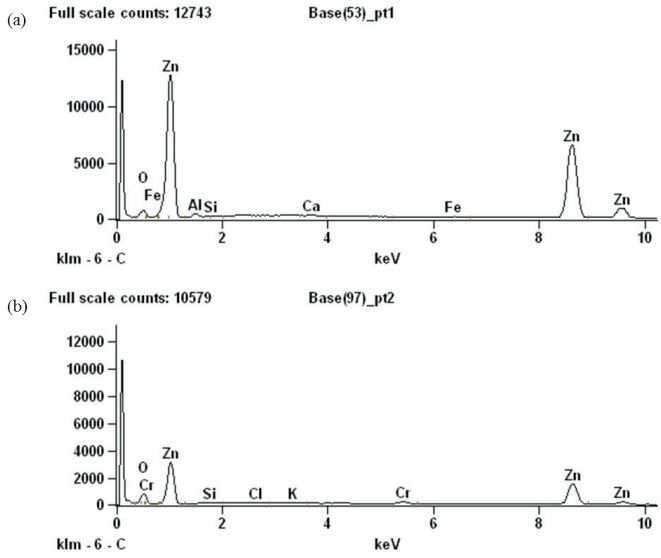

Fig. 4. EDS spectrum for (a) ZA1 and (b) ZC2 nanocomposite coatings

3.2. Structural and microhardness studies

XRD was used to study the effect of the incorporated nanoparticulates on the average crystallite size and crystallographic orientation on Zn matrix. The XRD patterns of Zn, ZA1 and ZC2 coatings obtained are shown in Figure 5. The major diffraction lines can be attributed to Zn hexagonal structure. The composites follows the same pattern but with different peak intensities. The modification in peak intensities indicates the presence of the nanoparticles in the coating. The peak width of the composites was also found be slightly broader than that of the matrix.

Full width at half maximum (FWHM) of (101) peak was then used to calculate the crystallite sizes of the coatings using Sherrer equation:

$$D = \frac{K\lambda}{BCos\theta}$$

Where D is the diameter of the crystal, K the Sherrer factor (≈1), λ radiation incident wavelength, B the line width and θ is the position for (101) peak.

The reinforcement of the coating with Al_2O_3 and Cr_2O_3 particles reduced the average crystallite size of the matrix from 31 to 15 and 28 nm respectively.

The incorporation of nanoparticles increases nucleation sites and thus disturbing crystal growth. Nanoparticles were also reported to adsorb on the growing crystal and impede its further growth resulting in smaller crystal sizes [3, 21].

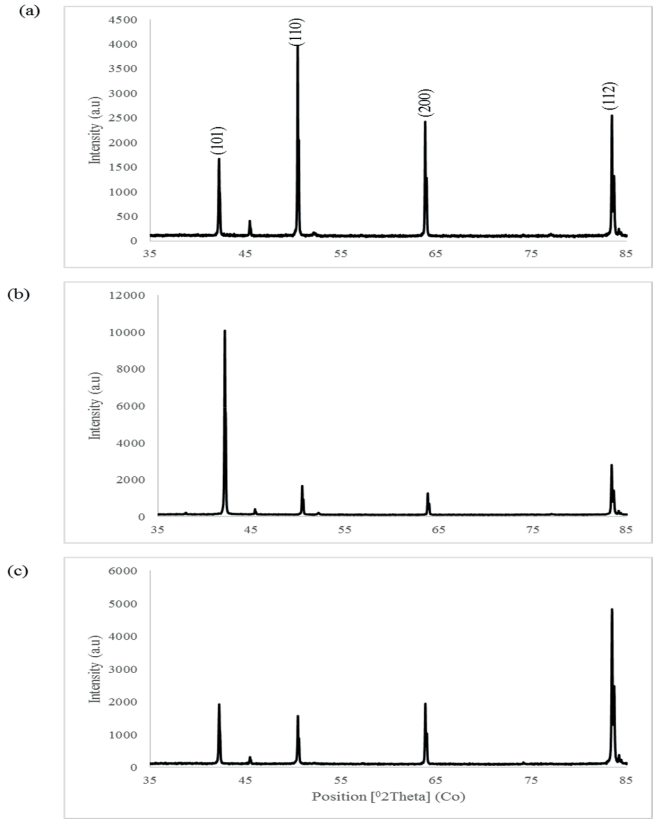

Fig. 5. X-ray diffractograms of (a) Zn coating, (b) ZA1 composite coating and (c) ZC2 composite coating

Figure 6 shows effect of bath particle concentration on the microhardness property of the coatings. It is evident from the figure that all the composite coatings exhibited improved microhardness values as compared to as received and plain Zn samples. Therefore, this result can be attributed to the incorporation of the nanoparticles into the Zn matrix. The presence of these particles in the coating hinders the crystal growth of Zn by increasing the number of nucleation sites and thus reducing the grain size. Several authors have reported similar results when these nanoparticles were incorporated into metal matrixes to form a composite alloy [7], [11]. Addition of5 g/l of Al_2O_3 nanoparticles into the electrolyte solution yielded maximum microhardness of 192 HV for ZA composite coatings. Further increment of the particles from 5 to 10 g/l had no significant influence in microhardness of the coatings. Loading of particles in the bath beyond optimal concentrations promotes agglomeration and reduce efficiency of uniform codeposition. This leads to generation of defects in the resultant deposits and hence the decrease in microhardness when the particle loading was increased to 10 g/l. On the other hand, increase of Cr_2O_3 particles from 10 to 20 g/l improved the microhardness from 161 to 228 HV. The improvement in microhardness yield obtained here is in agreement with Gugliemi's two step absorption model. The model states that increasing bath particle content increases the chance of particles to be codeposited at the cathode [13]. This suggests that coatings fabricated from baths containing high particle concentration contain the highest particle content and hence improved coating quality. Therefore, the 228 HV microhardness yield obtained can be attributed to the increased Cr_2O_3 particles in ZC2 composite coating.

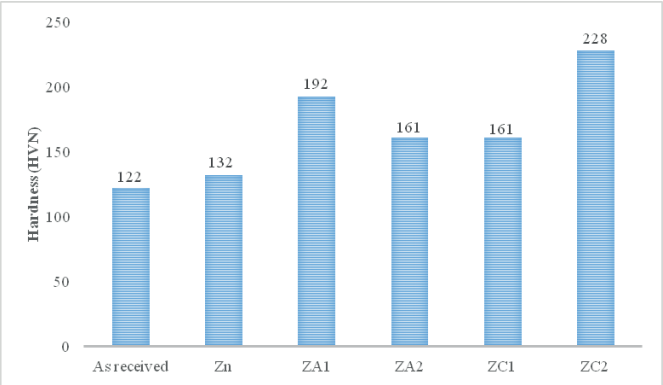

Fig. 6. Microhardness values for as received, Zn, ZA and ZC nanocomposite coatings

3.3. Corrosion studies

The polarization measurements to evaluate the corrosion behavior of the samples were carried out in a 3.65% NaCl environment under ambient conditions in a potential range of -1.5 to 1.5 V. Figure 7 shows the polarization curves of as received, Zn, Zn-Al_2O_3 and Zn-Cr_2O_3 nanocomposite coatings. A positive shift in potential can be observed for all the composite coatings when compared to as received sample. However, a different behavior was observed when the composite coatings were compared with Zn matrix. A negative potential shift was obtained for all the composites except for ZA1.Zn possesses good anti-corrosive properties and protect mild steel from corrosion attack when it is used as protective coating. The main constituent of all the composite coatings is also Zn. When 5g/L of Al_2O_3 was added into the bath to co-deposit on mild steel with Zn, an increase in potential from -1.1282 (Zn) to -1.0562 V (ZA1) was obtained. A substantial decrease in current density from 12.8 to 0.22 µA/cm^2 and increase polarization resistance from 0.957 to 4.16 kΩ corresponds with the positive shift in potential. These results can be attributed to the incorporation of Al_2O_3 nanoparticles into Zn matrix. Incorporation of these particles into the matrix has been reported to exhibit inhibiting effect on metal corrosion and thus enhancing corrosion resistance of the coatings.

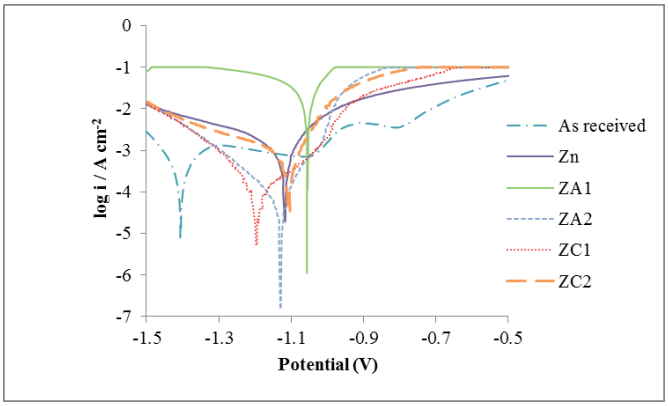

Fig. 7: Polarization curves of as received, Zn and Zn, ZA and ZC nanocomposite coatings in 3.65 wt.% NaCl solution

The uniform distribution of the nanoparticles in the Zn matrix fills the micro holes, pores and other surface defects that can promote exposure of the matrix to corrosive medium, and reduces the active sites for corrosion attack. However, further increase of the particles from 5 to 10 g/L in the bath yielded no positive results. This may be due to agglomeration of particles in the bath when they are added beyond optimal concentration leading to formation of non-uniform deposits. Blejan et al obtained similar results when Al_2O_3 particle loading exceeded the optimal concentration [6]. An improvement in corrosion resistance was observed when Cr_2O_3 nanoparticles concentration was increased from 10 to 20 g/L. A substantial decrease in current density from 47.8 to 10.7 µA/cm2 and increase in polarization resistance from 0.758 to 1.263 kΩ for ZC1 and ZC2 have been observed. However, this result poses no significance when compared with plain Zn. Therefore, ZA1 stands as the better coating compared to all the coatings.

TABLE 3
Extrapolated corrosion values obtained from Tafel plots

Sample	I_{corr} (A/cm²)	R_p (Ω)	E_{corr} (V)	Corrosion rate (mm/year)
As received	0.002761	55.565	-1.406	2.412
Zn	1.28E-05	957.57	-1.1282	0.012
ZA_1	2.22E-07	4160.74	-1.0562	0.0002
ZA_2	2.17E-05	846.52	-1.1382	0.017
ZC_1	4.78E-05	758.13	-1.1972	0.0515
ZC_2	1.07E-05	1263.8	-1.1075	0.007

3.4. Thermal stability

Evaluation of thermal stability of the nanocomposite coatings was conducted by exposing the samples to annealing temperature of 250 °C. Figure 8 shows the thermal behavior of the samples obtained after they were exposed to heat treatment for duration range of 0.5, 2 and 16 hours at 250 °C.

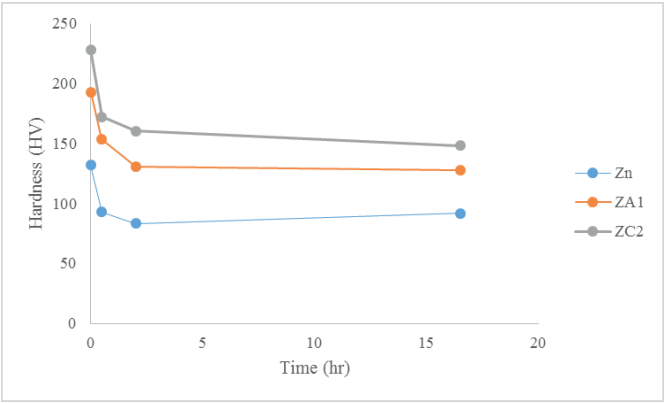

Fig. 8. Variation of microhardness of Zn, ZA1 and ZC2 deposits at 250°C for 0.5, 2 and 16 h.

The evaluation of the heat treated samples followed a microhardness evolution to determine their thermal stability. The figure shows a decrease in microhardness of all the samples with respect to time of exposure but the composites maintain higher values than that of Zn. These values are

maintained higher throughout the experiment. From the observed results, it can be deduced that the composites exhibit better thermal stability properties than Zn and this is attributed to the incorporation of the nanoparticles into Zn matrix. The incorporation of these nanoparticles into a metal matrix slows down grain growth and surface oxidation [14]. Notably, Zn-Cr_2O_3 can be seen to be more stable than Zn-Al_2O_3 indicating that Cr_2O_3 nanoparticles exhibit better thermal properties than Al_2O_3.

3.5. Tribological behavior

Figure 9 shows the wear performance of as received sample, Zn coating, Zn-Al_2O_3 and Zn-Cr_2O_3 nanocomposites which were tested at a constant normal load of 5 N for a maximum duration of 1000 seconds under dry reciprocating sliding conditions.

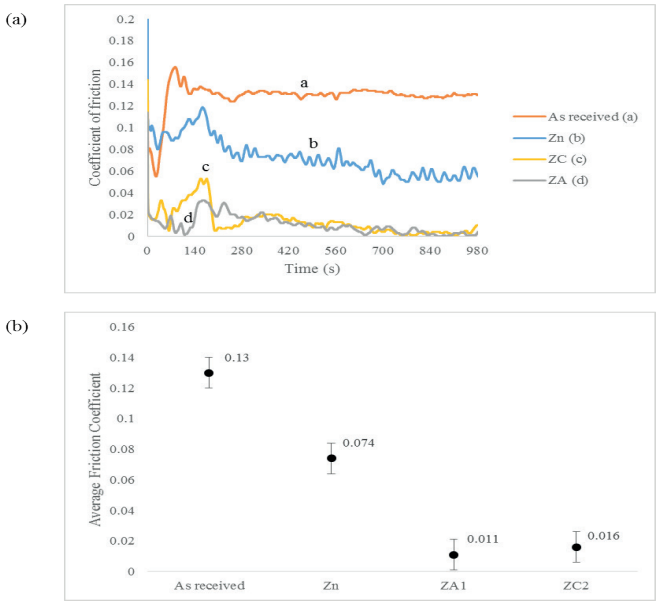

Figure 9:Friction coefficients (a) Friction coefficient vs time, (b) Average friction coefficients of as received, Zn, ZA1 and ZC2 nanocomposite coatings

The average friction coefficient values of the samples are presented in Figure 9(b). The figure reveals a decrease in coefficient of friction for all the coatings. The high coefficient of friction of as received sample (0.13) is reduced to 0.074 when the mild steel was coated with Zn. A further decrease to 0.011 and 0.016 are obtained when Al_2O_3 and Cr_2O_3were incorporated into Zn matrix respectively. These results suggest that the incorporated nanoparticles provide lubricating properties to Zn matrix by reducing direct contact of the tungsten carbide ball with metal matrix. ZA1nanocomposite coating exhibit the lowest coefficient of friction followed by ZC2. This indicates that Al_2O_3 particles possess better self-lubricating properties than Cr_2O_3 when incorporated to Zn matrix. Reduction in coefficient of friction results in lower mass loss due to wear. The results obtained by Lee showed a correlation between friction coefficient and mass loss; these two factors are directly proportional [17].

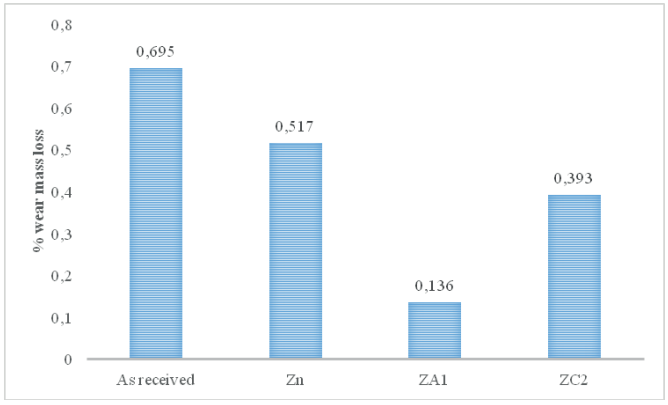

Fig. 10. Percentage wear mass loss of as received, Zn and Zn nanocomposite coatings obtained under dry sliding conditions at load of 5N and speed of 200 rev/min

The wear percentage loss values of as received, Zn, ZA1 and ZC2 are shown in Figure10. The figure shows that as received sample exhibit high wear loss (0.695 wt%) as compared to the all the coatings. Coating the sample with Zn reduced the wear loss of as received sample to 0.517 wt%. The inclusion of Al_2O_3 and Cr_2O_3 nanoparticles into the Zn matrix further reduced the wear loss to 0.136 and 0.393 wt% respectively. These results support the friction tests and prove that the incorporation of these nanoparticles have significant effect on the wear resistance of Zn coatings. The reduction in wear loss due to the incorporation of the nanoparticles can be attributed to the excellent self-lubricating properties exhibited by these nano-materials. A possible formation of a protective barrier between the wear media and the Zn matrix by the particles can also affect the wear behavior of the coatings. Al_2O_3 nanoparticles incorporation into Zn matrix showed to be the better materials to improve wear resistance as compared to Cr_2O_3 particles.

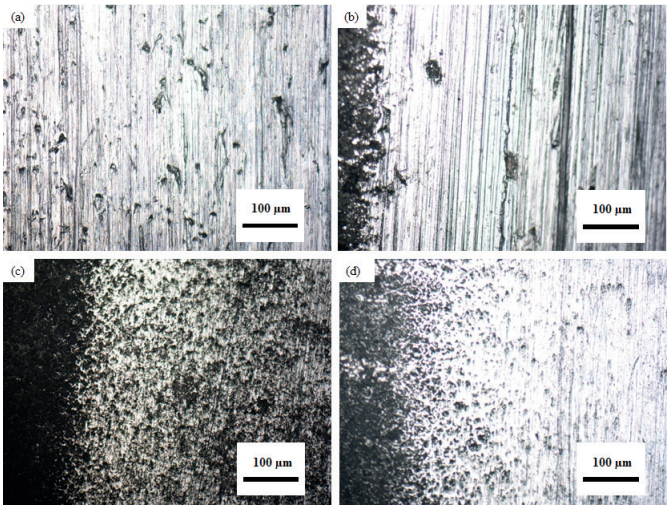

Fig. 11. Optical Microscope micrographs of worn out surfaces (a)as received sample, (a) Zn electrodeposits (c) ZA1 alloy and (d) ZC2 nanocomposite alloy

The surface morphology of the worn out samples have been investigated to study the nature of wear and the magnitude of damage caused by the wearing wheel. Figure11 shows the worn surface morphologies of as received sample, plain Zn

coating, Zn-Al_2O_3 and Zn-Cr_2O_3 nanocomposite coatings. The worn out surface of as received sample exhibit parallel micro-ploughing, microcracks and grooves as it can be observed in Figure11 (a). The nature of damage that has been caused on this sample during the wear tests suggest that the mechanism of wear associated with scars on the micrographs is mainly abrasive wear. Zinc coating (Fig. 11b) in the absence of additives shows a similar behavior as the as received sample but possesses fewer furrows, microcracks and grooves. The coating is also peeled from the substrate and the mild steel surface can be seen. The extents of damage of ordinary zinc as compared to as received sample suggest that the presence of Zn on the mild steel substrate reduced the wear mass loss. Partial peeling of the coating have been observed on the worn out surfaces of the nanocomposite coatings indicating the interface bonding strength between the composite and the substrate is stronger than that of plain Zn. This result also shows that the composite coatings exhibited better wear resistance as compared to as received and Zn coating. Therefore, the improved wear resistance of the composites can be ascribed to the presence of Al_2O_3 and Cr_2O_3 nanoparticles in the Zn matrix. ZA1 (Fig. 11c) shows less damage than ZC2 (Fig. 11d) and proves that Al_2O_3 particles have better self-lubricating properties than Cr_2O_3.

4. Conclusion

Zn-Al_2O_3 and Zn-Cr_2O_3 nanocomposite coatings were successfully fabricated using electrodeposition technique in chloride bath solution. The effect of the incorporated nanoparticles on the surface morphology, microhardness, corrosion resistance, thermal stability and wear properties were studied and compared. Scanning electron microscope micrographs showed that both Al_2O_3 and Cr_2O_3 have significant effect on the morphology of the coatings and EDS confirmed the presence of the nanoparticles. Al_2O_3 incorporation improved the corrosion resistance while Cr_2O_3 had no significant effect on the anti-corrosive properties of Zn matrix. Zn-Cr_2O_3 composite exhibited better microhardness and thermal stability than Zn-Al_2O_3 composite coating. Zn- Al_2O_3 possessed better self-lubrication properties and hence better tribological behavior. Therefore, it can be concluded that Zn-Al_2O_3 composites are suitable for wide industrial applications where the coatings are expected to perform under chemical, thermal and mechanical demanding conditions. However, Zn-Cr_2O_3 is limited to industries that require the coatings for their mechanical properties only.

Acknowledgements

This material is based upon work supported financially by the National Research Foundation. The equipment support by Surface Engineering Research Centre (SERC) Tshwane University of Technology, Pretoria is deeply appreciated.

REFERENCES

[1] Z.F. Lodhi, J.M.C. Hovestad, H. Terryn, J.H.W. deWit, Surf. Coat Tech. **202**, 84–90 (2007).
[2] W.S. Khan, R. Asmatulu, Nano. Saf. **20**, 1-16 (2013).
[3] K. Vathsala, T.V. Venkatesha, App. Surf. Sci. **257**, 8929-8936 (2011).
[4] S. Ranganatha, T.V. Venkatesha, K. Vathsala, M.K. Punith kumar, Surf. Coat. Tech. **208**, 64-72 (2012).
[5] X. Xia, I. Zhitomirsky, J.R. McDermid, J. of mat. Proc. Tech. **209**, 2632–2640 (2009).
[6] D. Blejan, L. M. Muresan, Mat. Corr. **63**, 999-1020 (2009).
[7] H. Zheng, M. An, J. of Alloys and Compds **459**, 548–552(2008).
[8] J. Fustes, A. Gomes, J. of Sol. State. Electro.**12**, 1435–1443(2008).
[9] B.M. Praveen, T.V. Venkatesha, Int. J. of Electrochem. doi:10.4061/2011/261407 (2011).
[10] O. Hammami, L. Dhouibi, P. Bercot, E. Rezrazi, E.Triki, Int. J. of Corr. **12**, 18-24 (2011).
[11] O.S.I. Fayomi, A.P.I. Popoola, C.A. Loto, Int. J. of Electrochem. Sci. **9**, 885-3903 (2014).
[12] M. Srivastava, J.N.Balaraju, B. Ravishankar, K.S. Rajam, Surf. Coat. Tech. **205**, 66-75 (2010).
[13] N. Guglielmi, J. of Electrochem. Soc. **119**, 1009–1011(1972).
[14] I. Apachitei, F.D. Tichlaar, J. Duszczyk, L. Katgerman, Surf. Coat. Tech. **149**, 263-278 (2002).
[15] L. Kong, Q. Bi, S. Zhu, J. Yang, W. Liu, Trib. Int. **45**, 43-49 (2012).
[16] C.S. Ramesh, S.K. Seshadri, Wear, **255**, 893-902 (2003).
[17] C.K. Lee, Trib. Int. **55**, 7-14 (2012).
[18] H.B. Hassan, Z. Abdel Hamid, Int. J, of hydr. energy, **36**, 5117-5127 (2011).
[19] Z. Dong, X. Peng, Y. Guan, F. Wang, Corr. Sci. **62**, 147-152 (2012).
[20] O. Sancakoglu, O. Culha, M. Toparli, B. Agaday, E. Celik, Mat. and Des. **32**, 4054-4061(2011).
[21] S. Srikomol, P. Janetaisong, Y. Boonyongmaneera, R. Techapiesancharoenki, Ach. Met and Mat, **59**, 1287-1292 (2014)